Scientific Journal of Silesian University of Technology. Series Transport
Zeszyty Naukowe Politechniki Śląskiej. Seria Transport

Volume 131 **2026**

p-ISSN: 0209-3324

e-ISSN: 2450-1549

DOI: https://doi.org/10.20858/sjsutst.2026.131.12

Journal homepage: http://sjsutst.polsl.pl

Article citation information:
Rzydzik, S., Panfil, W., Myszor, D., Cyran, K., Moczulski, W. Improvement of the agility and manageability of an autonomous blimp. *Scientific Journal of Silesian University of Technology. Series Transport*. 2026, **131**, 189-205. ISSN: 0209-3324.
DOI: https://doi.org/10.20858/sjsutst.2026.131.12

Sebastian RZYDZIK[1], Wawrzyniec PANFIL[2], Dariusz MYSZOR[3], Krzysztof CYRAN[4], Wojciech MOCZULSKI[5]

IMPROVEMENT OF THE AGILITY AND MANAGEABILITY OF AN AUTONOMOUS BLIMP

Summary. This paper presents the development and experimental validation of a control-oriented numerical model and a PID-based autonomous control system for an unmanned blimp. A simplified dynamic model was implemented in the GNU Octave environment and used for the systematic tuning of vertical and horizontal propulsion controllers. Experimental identification using a full-scale blimp prototype demonstrated good agreement between simulated and real flight responses, with mean time errors below 5% and altitude errors below 1% in representative vertical maneuvering experiments. Indoor flight tests performed with a Pixhawk autopilot confirmed stable autonomous altitude control, with steady-state altitude deviations limited to approximately 4-5 cm, as well as reliable

[1] Silesian University of Technology, Faculty of Mechanical Engineering, Konarskiego Str. 18A, 40-100 Gliwice, Poland. Email: sebastian.rzydzik@polsl.pl. ORCID: https://orcid.org/0000-0003-3352-3986
[2] Silesian University of Technology, Faculty of Mechanical Engineering, Konarskiego Str. 18A, 40-100 Gliwice, Poland. Email: wawrzyniec.panfil@polsl.pl. ORCID: https://orcid.org/0000-0001-7304-554X
[3] Silesian University of Technology, Faculty of Automatic Control, Electronics And Computer Science, Akademicka Str. 16, 40-100 Gliwice, Poland. Email: dariusz.myszor@polsl.pl. ORCID: https://orcid.org/0000-0002-5764-6246
[4] Silesian University of Technology, Faculty of Automatic Control, Electronics And Computer Science, Akademicka Str. 16, 40-100 Gliwice, Poland. Email: krzysztof.cyran@polsl.pl. ORCID: https://orcid.org/0000-0003-1789-4939
[5] Silesian University of Technology, Faculty of Mechanical Engineering, Konarskiego Str. 18A, 40-100 Gliwice, Poland. Email: wojciech.moczulski@polsl.pl. ORCID: https://orcid.org/0000-0002-4697-1561

target-point acquisition during autonomous navigation. The results demonstrate that the proposed numerical model enables fast and effective controller tuning while maintaining sufficient accuracy for real-world implementation and that the tuned PID controllers provide stable, smooth, and repeatable autonomous flight suitable for inspection and monitoring applications.

Keywords: inspection and monitoring, autonomous airship, control system, virtual teleportation

1. INTRODUCTION

There is a growing trend of using unmanned aerial vehicles (UAVs) for sustained inspection and monitoring operations. Illustrative examples include the surveillance of sporting events, such as football matches; large-scale cultural events, such as outdoor concerts; and the inspection of expansive infrastructure, such as railway lines and highways. In such scenarios, where UAVs are often limited by constrained energy resources, contemporary airships are poised to assume an increasingly significant role. Recognizing this potential, the SkyTech Products Research and Development team has launched a research initiative with the objective of developing a ground-based remote-control station for UAVs, with airships representing a primary category.

A review of the existing literature indicates that while advanced airship control strategies and high-fidelity dynamic models have been widely investigated, there remains a practical need for control-oriented numerical models that support the implementation and tuning of classical controllers in real aerial blimps. In particular, despite the widespread use of PID control in airship applications, the criteria and conditions for its tuning are often not explicitly discussed.

Therefore, the objective of this paper is to develop a simplified numerical model of an unmanned airship suitable for control design and to implement and tune PID controllers for vertical and horizontal propulsion systems. The proposed approach focuses on achieving stable and reliable maneuvering behavior under representative operating conditions.

This paper presents the development process of a dedicated autopilot algorithm and its implementation in software specially geared to aerial blimps. It is composed as follows: Section 3 describes a numerical model, which is further implemented in the GNU Octave simulation environment. Section 4 shows an implementation of the control algorithms on a real unmanned airship. To this end, a well-known PixHawk autopilot module has been implemented. The next section deals with exhaustive experiments whose goal has been to estimate and tune different parameters of the developed model. Several scenarios have been proposed, and then proper experiments were carried out whose results were analyzed to yield basic statistics characterizing inherent data deviation. Then, in Section 6, an experimental verification of the control algorithms is shown. The article ends with conclusions.

2. LITERATURE REVIEW

The field of aviation, long dominated by fixed-wing aircraft and rotary-wing helicopters, is witnessing the resurgence of a unique aerial platform: the airship [8, 1]. These lighter-than-air vehicles, buoyed by gases such as helium, possess inherent advantages that are driving renewed interest in their development and deployment. Unlike heavier-than-air platforms, airships excel in endurance, offering prolonged flight times and efficient hovering [12]. This characteristic enables a wide range of applications, from persistent surveillance and long-haul cargo transport to indoor inspections and entertainment robotics [4, 5]. However, the interaction of airships with aerodynamic forces and the challenge of achieving precise control introduce significant engineering difficulties that require advanced solutions [13].

This review of airship control systems reveals a field combining established principles with modern innovations. The fundamental challenge lies in effectively governing airship motion, enabling navigation in three-dimensional space, maintaining orientations, and executing complex maneuvers with accuracy and reliability [1, 8]. Meeting these requirements demands a thorough understanding of airship dynamics, acting forces, and robust control algorithms capable of translating commands into precise actuator responses.

A major difficulty in airship control arises from their inherent underactuation. In contrast to multirotor drones that can control all degrees of freedom independently, airships typically have fewer control inputs than controlled motions [13]. As a result, certain movements are coupled and cannot be controlled directly; for example, lateral motion often requires prior rotation. This characteristic increases control complexity and necessitates advanced strategies to ensure stability and performance.

Environmental disturbances further complicate control tasks. Due to their large surface area, airships are highly sensitive to wind effects, including gusts and turbulence, which can significantly disrupt motion and trajectory tracking [8, 9, 13]. Consequently, control systems must be robust and adaptive to maintain safe and reliable operation under varying atmospheric conditions.

The physical design of the airship also strongly affects controllability. Parameters such as hull shape, size, and mass distribution directly influence dynamic behavior [4, 12]. Research has examined various geometries to balance aerodynamic efficiency and maneuverability, with studies highlighting the role of the slenderness ratio in stability and performance [12]. Alternative configurations, including spherical blimps equipped with tetrahedrally arranged thrusters, have been proposed to enhance agility and enable omnidirectional motion [4].

Application-driven research continues to expand. Indoors, compact and highly maneuverable airships are considered for tasks requiring safe operation near obstacles or humans, such as confined-space inspections, vertical farm monitoring, and interactive entertainment [5, 12]. Emphasis is placed on precise low-speed motion, stable hovering, and collision avoidance. The BlimpleBee platform exemplifies this development trend, demonstrating the feasibility of helium-assisted vehicles for delicate inspection missions [4].

For outdoor missions, priorities shift toward endurance, payload capacity, and robustness to weather disturbances. Autonomous airships are envisioned for long-term surveillance, environmental monitoring, and cargo transport, offering efficiency advantages over conventional drones [8, 12]. These applications impose stringent requirements on control systems, including disturbance rejection, long-range navigation, and reliable stability.

Safety and reliability are particularly critical when airships operate near people or in hazardous environments, such as disaster response scenarios [4]. Hybrid platforms that combine lighter-than-air properties with multirotor redundancy, such as the Janus system, address these concerns by enabling fallback flight modes in case of buoyancy failure [11].

To tackle the diverse challenges of airship control, researchers have explored a broad range of methodologies. Classical approaches, including PID control, remain widely used due to their simplicity and effectiveness for basic stabilization tasks [1, 8]. Nonetheless, their limitations in nonlinear and uncertain environments have motivated the adoption of advanced strategies.

Adaptive control allows online parameter adjustment to compensate for model uncertainties, while robust control methods guarantee stability under bounded disturbances [13]. Model

Predictive Control (MPC) exploits future-state predictions to optimize control actions, and intelligent approaches, such as reinforcement learning, are increasingly investigated to enable learning-based adaptation to complex environments [8].

Accurate dynamic modeling is a prerequisite for controller development and validation. This involves capturing buoyancy, aerodynamic forces, and in some cases tether interactions [1, 9]. Mathematical models derived from stability derivatives and computational fluid dynamics (CFD) analyses are commonly used for simulation-based controller design [12].

Despite extensive research on airship aerodynamics and advanced control strategies, fewer studies address the practical implementation and tuning of classical controllers based on control-oriented numerical models. In particular, systematic procedures for selecting PID gains in underactuated airship systems remain insufficiently documented.

Motivated by this gap, the present study focuses on developing a numerical model suitable for closed-loop simulations and investigating the implementation and tuning of PID controllers for vertical and horizontal motion control of an unmanned airship.

3. NUMERICAL MODEL

3.1. Mathematical model

The development of the numerical model began with an analysis of existing mathematical models of blimps, including both kinematic and dynamic formulations. A brief overview of the adopted modeling assumptions is presented below.

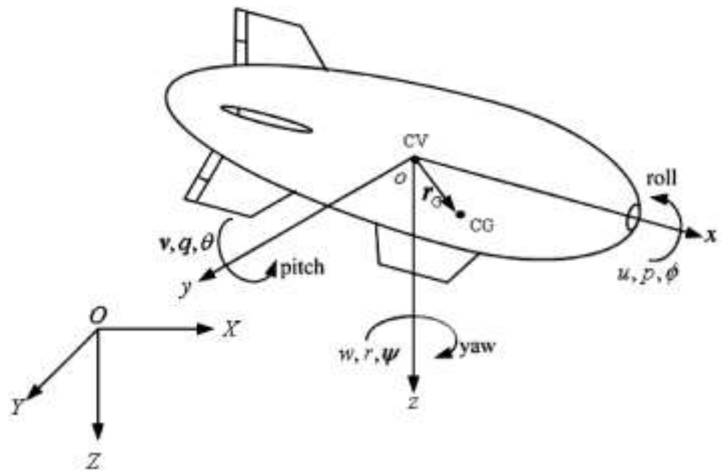

Fig. 1. Reference frames and motion parameters of the blimp [14]

Based on the reference frames shown in Fig. 1, the inertial coordinate system is defined as follows: the x-axis points to True North, the y-axis points east, and the z-axis points downward. The linear velocity components in the body-fixed frame are denoted by u (longitudinal), v (lateral), and w (vertical). The Euler angles are defined as θ (pitch), ϕ (roll), and ψ (yaw), while the angular velocity components are denoted by p, q, and r, corresponding to roll, pitch, and yaw rates, respectively.

The kinematic equations of motion of the blimp can be expressed as

$$\begin{bmatrix} \dot{P} \\ \dot{\Omega} \end{bmatrix} = \begin{bmatrix} S_1 & 0_{3\times3} \\ 0_{3\times3} & S_2 \end{bmatrix} \begin{bmatrix} v \\ \omega \end{bmatrix}, \tag{1}$$

Where:

$$P = [x\, y\, z]^T$$

is the position vector in the inertial frame,

$$v = [u\, v\, w]^T$$

is the linear velocity vector expressed in the body-fixed frame,

$$\Omega = [\phi\, \theta\, \psi]^T$$

is the vector of Euler angles, and

$$\omega = [p\, q\, r]^T$$

is the angular velocity vector. The matrices $S_1$and S_2represent the rotation matrix and the kinematic transformation matrix, respectively.

The dynamic behavior of the airship is described using the Newton-Euler formalism

$$F = m\big(\dot{v} + \omega \times v + \dot{\omega} \times r_g + \omega \times (\omega \times r_g)\big), \tag{2}$$

$$\tau = I_0\dot{\omega} + \omega \times (I_0\omega) + m\, r_g \times (\dot{v} + \omega \times v), \tag{3}$$

where F and τ denote the resultant external forces and moments acting on the vehicle, including aerodynamic forces, buoyancy, gravity, and propulsive thrust. The vector

$$r_g = [x_g\, y_g\, z_g]^T \tag{4}$$

represents the displacement of the center of gravity (CG) relative to the center of volume (CV). The inertia tensor with respect to the origin of the body-fixed frame is defined as

$$I_0 = \begin{bmatrix} I_x & -I_{xy} & -I_{xz} \\ -I_{yx} & I_y & -I_{yz} \\ -I_{zx} & -I_{zy} & I_z \end{bmatrix} \tag{5}$$

with the symmetry conditions $I_{xy} = I_{yx}$, $I_{xz} = I_{zx}$, and $I_{yz} = I_{zy}$.

The mass m in Eqs. (2)-(3) denotes the total effective mass of the airship, including the envelope, gondola, propulsion system, and payload.

The total mass and inertia were modeled as sums of rigid-body and added-mass contributions

$$m = m_{RB} + m_A, I_0 = I_{RB} + I_A,$$

where m_{RB} and I_{RB} are the rigid-body mass and inertia tensor, while m_A and I_A represent the added mass and added inertia arising from the acceleration of the surrounding air.

The added-mass terms were estimated using an ellipsoidal approximation of the airship envelope. The hull was approximated as a prolate spheroid whose principal axes correspond to the longitudinal and transversal dimensions of the envelope. Under the assumption of inviscid potential flow, the added mass and added inertia coefficients were determined as functions of the airship geometry and the displaced air volume.

The added-mass and added-inertia contributions were incorporated directly into the effective mass and inertia terms in Eqs. (2)-(5). This formulation is well suited for maneuvering simulations and ensures a physically consistent representation of translational and rotational fluid-structure interaction effects.

Further details of the mathematical background and parameter estimation methods can be found in [2, 6, 7, 10, 14].

The main objective of this study was the implementation and tuning of PID controllers for the vertical and horizontal propulsion systems. For vertical motion control, the following control law was applied:

$$u_z = K_{ph} e_z + K_{ih} \int e_z \, dt - K_{dh} \dot{z}, \tag{6}$$

where u_z is the vertical thrust ratio, e_z is the altitude error, $\dot{z}$ is the vertical velocity, and K_{ph}, K_{ih}, and K_{dh} are the proportional, integral, and derivative gains, respectively.

Yaw motion was controlled by differential thrust of the horizontal propellers

$$u_r = K_{pv} e_\psi + K_{iv} \int e_\psi \, dt - K_{dv} \dot{\psi}, \tag{7}$$

$$u_l = K_{pv} e_\psi - K_{iv} \int e_\psi \, dt + K_{dv} \dot{\psi}, \tag{8}$$

where u_r and u_l denote the right and left thrust ratios, e_ψ is the yaw angle error, $\dot{\psi}$ is the yaw rate, and K_{pv}, K_{iv}, and K_{dv} are the controller gains.

3.2. Implementation of the blimp numerical model

The numerical model incorporates the following elements:

- geometric properties, such as longitudinal and transversal cross-section dimensions;
- mass properties, including mass distribution and moments of inertia;
- thruster characteristics, specifically thrust generation;
- aerodynamic properties, such as drag coefficients;
- external disturbances, including wind direction and speed.

The aerodynamic forces were modeled using a simplified quasi-static formulation. The drag forces along the principal body axes were assumed to be proportional to the corresponding velocity components. Lift and side-force effects were neglected due to the low operating speeds and small angles of attack considered in the simulations. This level of modeling detail was found sufficient for control design and performance evaluation purposes.

The model was developed based on the approaches described in [2, 3] and implemented using the ode45 solver. With appropriate solver configuration, the model generates time histories of key state variables, including spatial position, Euler angles (yaw and pitch), thrust commands for vertical and horizontal propellers (left and right), linear velocities, and angular velocities.

The PID controller parameters were selected based on closed-loop simulation studies. The tuning criteria included stability of the airship motion, acceptable settling time, limited overshoot in altitude and yaw responses, and smooth actuator commands within admissible thrust limits. The parameters were adjusted under representative operating conditions relevant to low-speed maneuvering tasks.

Simulation results obtained using the numerical model are presented in the second part of this paper.

4. INTEGRATION OF THE BLIMP CONTROL MODEL WITH PIXHAWK AUTOPILOT

4.1. Geometrical properties of the blimp prototype

Figure 2 shows the physical blimp prototype used in this study, while Figure 1 presents a schematic representation of the adopted reference frames and motion parameters.

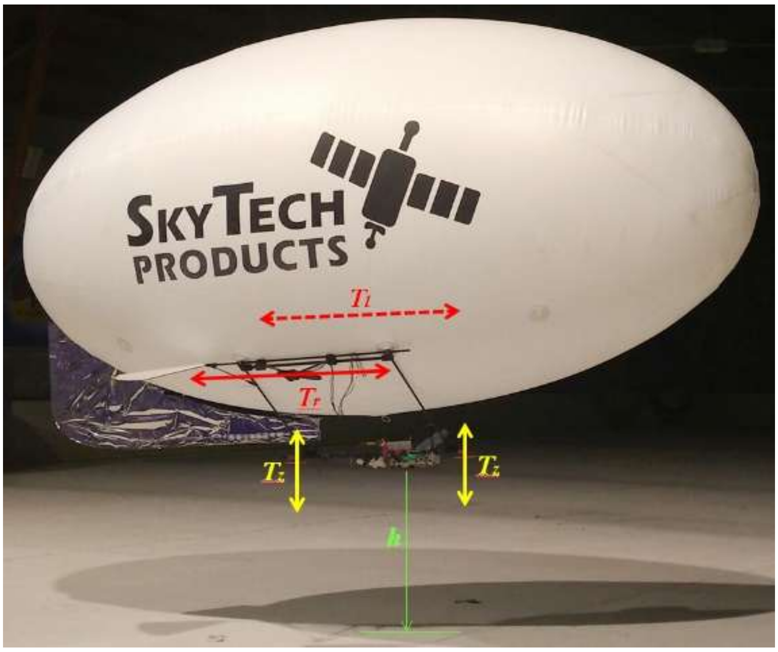

Fig. 2. The blimp prototype: T_r – right horizontal thrust, T_l – left horizontal thrust, T_z – vertical thrust

The geometry of the airship envelope was approximated using an ellipsoidal model, consistent with the schematic representation shown in Fig. 1. The hull can be described as a prolate spheroid with semi-axes a, b, and c, where $a$corresponds to the longitudinal axis and $b = c$to the transversal axes. For the prototype used in this study, the overall length of the envelope was approximately $L = 4.0$ m, while its maximum diameter was approximately $d = 2.0$ m. This corresponds to semi-axes $a = 2.0$ mand $b = c = 1.0$ m, yielding a slenderness ratio $L/d = 2.0$.

These geometric parameters were used to estimate the displaced air volume and to determine the added-mass and added-inertia coefficients employed in the numerical model. The ellipsoidal approximation provides a reasonable balance between physical accuracy and computational simplicity and is commonly adopted in control-oriented modeling of airships.

The stabilizing surfaces visible in Fig. 1 represent simplified tail fins intended primarily to enhance passive directional stability. Due to their small size and integration with the envelope, these surfaces are not clearly distinguishable in the photograph of the prototype shown in Fig. 2. In the current configuration, active control authority is provided exclusively by the vertical and horizontal propellers, while the stabilizing surfaces contribute only to passive aerodynamic damping and static stability effects, which are implicitly represented in the simplified aerodynamic model.

4.2. The idea of autonomous control

Figure 3 presents the conceptual architecture of the autonomous control system implemented for the blimp.

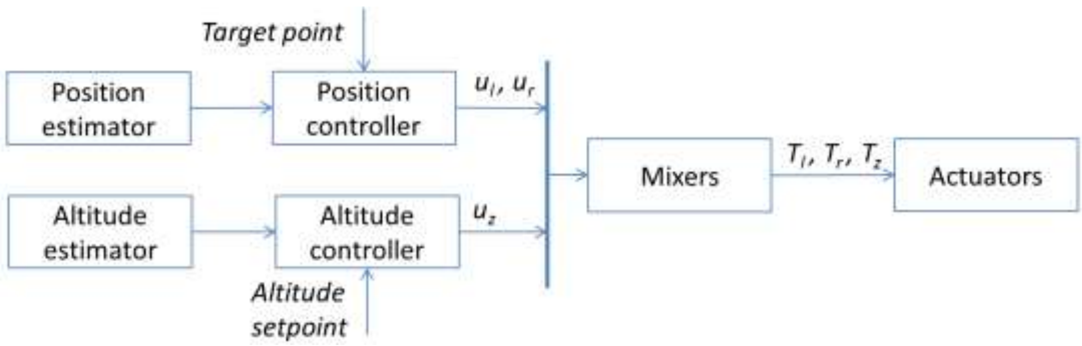

Fig. 3. Idea of an autonomous control system

The control of the flight consists of two independent control loops:

1) Vertical movement control – the height of the blimp above the ground (altitude) is continuously controlled by vertical thrust (T_z) and based on:
   a) altitude error calculated from the measurement of distance to the ground (h) using a laser distance sensor mounted on the bottom of the nacelle;
   b) vertical speed obtained by numerical differentiation of the altitude measurement (h) or directly from the IMU in the Pixhawk.
2) Horizontal movement control – the horizontal position of the blimp is continuously controlled by the left (T_l) and right (T_r) thrusts and based on the following:
   a) horizontal position error calculated from the actual GPS data and target point;
   b) angle error calculated from the compass data, actual and target point;
   c) yaw rate calculated from the gyroscope data – however, this information is not used at this stage and will be incorporated in future work.

4.3. Autonomous flight controller

The blimp control system was implemented using a Pixhawk flight controller. A dedicated module, named *blimp_control*, was developed in accordance with the PX4 Development Guide.

In the standard PX4 *Airship* configuration, thrust vectoring is handled within the mixer, allowing tilting actuators to simultaneously affect multiple motion axes. This results in a coupled control structure. In contrast, the proposed control system is tailored to the specific blimp configuration and employs a decoupled approach: two fixed horizontal propellers generate forward motion and yaw through differential thrust, while dedicated vertical propellers independently regulate altitude. This separation simplifies the control design and improves the transparency of the control structure.

The *blimp_control* module:

1) implements a PID controller for vertical motion (altitude) control;
2) implements a simplified rule-based controller for horizontal motion and navigation. A PID-based controller, previously developed and validated in numerical simulations (see Section 3), is planned to be implemented in future work.

The *blimp_control* module uses a set of configurable parameters that can be adjusted in real-time using QGroundControl via the MAVLink communication protocol, without the need to reprogram or restart the autopilot.

5. EXPERIMENTS FOR TUNING MODEL PARAMETERS

The identification of the blimp parameters consisted of:

1) Development of experiments scenarios.
2) Conduct experiments using the physical blimp model.
3) Analysis of the measurement results.
4) The choice of the parameter values for the mathematical model.

5.1. Scenarios of experiments

The purpose of the development of scenarios was to measure the response of the parameter values of the physical blimp model to known values of external impacts. The description of one of four example scenarios is presented below.

Tab. 1

Scenario example

Name	Changing the vertical thrust to the opposite
Stages	1. Place the blimp at a height of about 1 m. 2. Free the blimp and simultaneously run the vertical thrust fan (VFan) at 20% for 8 s. 3. Then, after 8 s from the beginning of the experiment, run the vertical thrust fan (VFan) at -20% for 4 s. 4. Leave the blimp until it falls to ground level.
Expected behavior	1. The blimp should lower its initial height. 2. Then, the blimp should increase its height, even after turning off the fan of the vertical thrust. 3. After the reverse vertical thrust is turned on, the blimp should quickly reduce its height (even when the fan is turned off) until the ground level is reached.

Observed features	1. Maximum altitude measured from the ground. 2. The time to climb to the maximum altitude and the time to descend from the maximum altitude to the ground level.
Comments	If the expected behavior of the blimp is not consistent with the description, it is possible to extend or shorten the duration of the vertical thrust of the fan, or reduce the thrust.

5.2. Results of experiments using the real blimp model

The scenario described above was the basis for conducting experiments on the real model of a blimp. Each experiment was performed 10 times, and the obtained data were subjected to statistical analysis (see Tab. 2). The following features have been recorded:

- horizontal and vertical thrust;
- unbalance weight;
- starting altitude;
- maximum altitude;
- time of positive and negative thrust;
- time of climb; and
- fall time.

Tab. 2

Summary of the statistical analysis of experimental data

	Vertical thrust [g]	Unbalanced mass [g]	Starting altitude [m]	Maximum altitude [m]	Duration of positive thrust [s]	Climb time [s]	Duration of negative thrust [s]	Descent time [s]
Average	62,7	18,2	1	5,43	8,4	8,5	5,0	22,8
Std. deviation	1,27	3,31	0	0,36	0,19	0,17	0,72	2,89

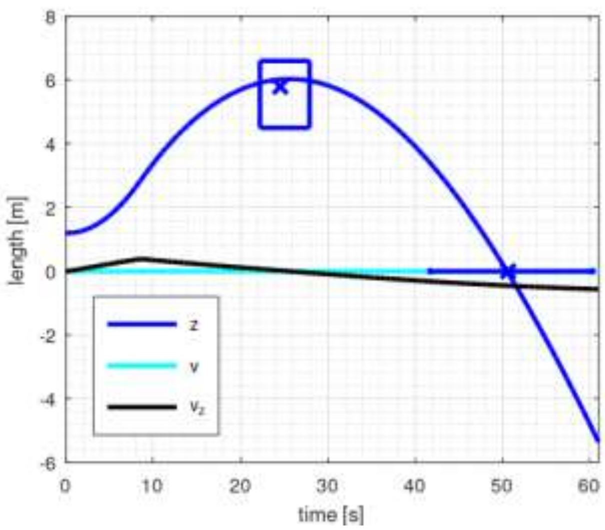

Fig. 4. The result of tuning the numerical model with the estimated error

5.3. Tuning of the blimp numerical model

The aim of the numerical model tuning process was to adjust its parameters to the values of the features measured during the experiments using the real blimp model. The basic criterion was to minimize the time and distance errors for each experiment, assuming the same values as the numerical model of the blimp. The example of tuning characteristics, in the case of changing the vertical thrust to the opposite, is shown in Fig. 4. In this experiment, the mean time error is equal to 4.84% (2.16[s]) and the mean z-length error (height) is equal to -0.43% (0.024[m]).

5.4. Examples of simulations using the controller numerical model

In the case of the vertical thrust controller, the mission focused on maintaining the flight altitude at 15-7.5-15 [m], with variable wind in the range <-1; 1> [m/s]. The results for the vertical thrust PID controller model with "soft" settings, for $K_{pv} = 0.2, K_{iv} = 0.16, K_{dv} = 4.8$, have been shown in Fig. 5.

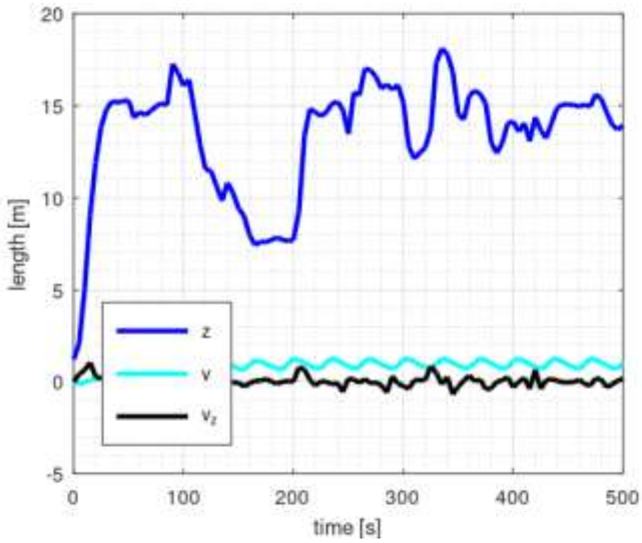

Fig. 5. The result of the numerical simulation: keeping altitude with wind

In the case of the horizontal thruster controller, the purpose was to fly in proximity of four points, defining a square under a side of 30 [m], with the assumption of lack of wind. The results of this simulation are shown in Fig. 6. The flight time was set at 500 [s]. PID parameters: $K_{ph} = 0.35$, $K_{ih} = 0.1$, $K_{dh} = 0.70$.

The results of a similar mission as before, but in the case of variable wind in the range of <-1; 1> [m/s], are shown in Fig. 7.

6. EXPERIMENTAL VERIFICATION OF AUTONOMOUS CONTROL OF THE BLIMP

6.1. Balancing the blimp

During the experiments, it was observed that the helium inside the envelope of the blimp evaporates over time. In consequence, the blimp becomes unbalanced, i.e., overloaded. It is extremely important to keep the blimp well balanced when developing altitude control algorithms. To do that, a bottle filled with salt has loaded the blimp. The amount of salt was constantly monitored.

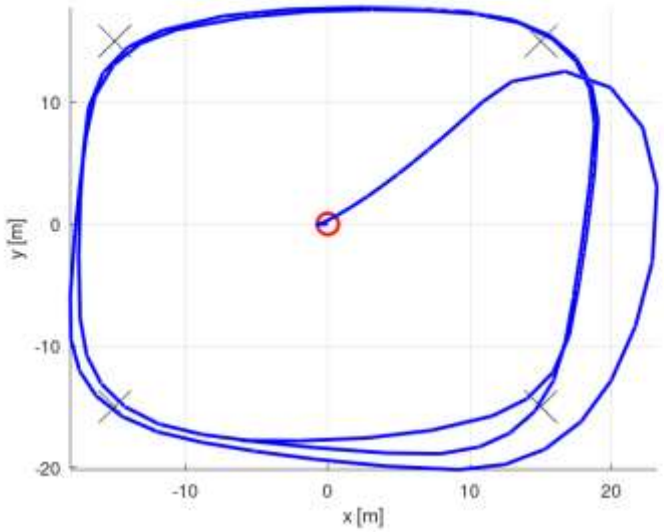

Fig. 6. The result of numerical simulation: flying in the proximity to four points without wind

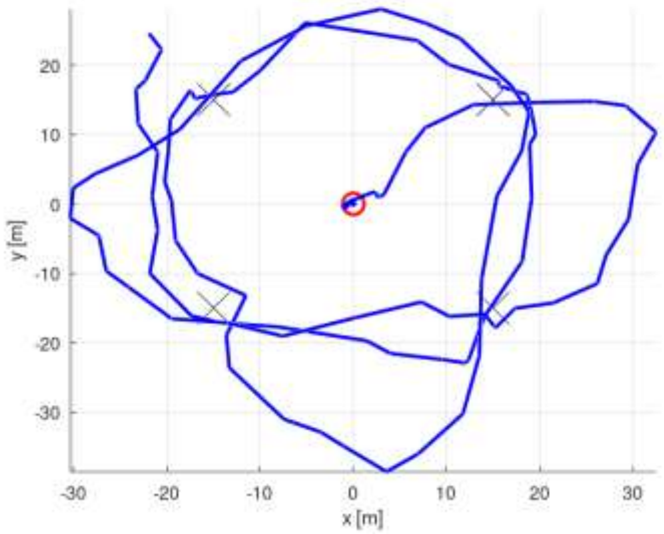

Fig. 7. The result of a numerical simulation: flying in proximity to four points in windy conditions

6.2. Experiments leading to the development of autonomous altitude control

Many experiments were carried out that led to final development and implementation of the elaborated (within numerical experiments, see Section 2) PID algorithm for vertical autonomous control. All these experiments took place inside the Ice Skating Hall of the Silesian University of Technology in Gliwice, Poland (Fig. 8). Exemplary experiments are discussed below and are documented in videos (available on the YouTube channel Blimp Experiments: https://www.youtube.com/playlist?list=PL-0gX2KowkKvQRTEmx0E84VluRMJ6jUTW) – it is recommended to enable audio playback when watching these videos.

The exemplary experiments are as follows:

1) Autonomous altitude control [video: 1_AutoHeight]

In this experiment, the blimp hovers at a specified altitude, i.e., 1.25 [m]. The following PID parameters were applied ($K_{pv} = 0.1$, $K_{iv} = 0.25$, $K_{dv} = 0.8$). These parameters were predetermined within numerical experiments.

Observations/conclusions: When the blimp is well balanced, the vertical propellers almost do not work. Over time, when the airship becomes increasingly unbalanced, the propellers spin faster and faster.

Fig. 8. Experimental verification of autonomous control

2) Flying up to the altitude setpoint [video: 2_AutoHeightFromBottom]

In this experiment, the blimp is released below a desired altitude (1.25 [m]) and flies up. Then it maintains the altitude. The same PID parameters as in experiment 1.

Observations/conclusions: at the beginning, the blimp is underloaded and flies up to the desired altitude. We can observe that the propellers do not work even below the given altitude because the D part of the PID controller takes into account the vertical speed of the blimp. When the blimp is close to the given altitude, the controller tries to “defend” against excessive crossing of a given point – it was observed when the blimp both flies up and down. Then the blimp hovers very well.

3) Flying to altitude setpoint [video: 3_AutoHeightFromTop]

In this experiment, the blimp is released above the desired altitude (1.25 [m]) and flies down. Then it maintains the altitude. The same PID parameters as in experiment 1.

Observations/conclusions: we can observe that at the beginning the propellers work very hard because the blimp is underloaded. Then the propellers stop working or even try to raise the blimp because the D part of the PID controller takes into account the vertical speed of the blimp - the controller tries to ‘defend’ against excessive crossing of a given point. Then the blimp hovers very well.

4) Autonomous altitude control (with ‘mild’ PID parameters) [video: 4_AutoHeightMildPID]

In this experiment, the blimp starts at 1.25 [m], then flies up to 2.25 [m] and then flies back (down) to 1.25 [m]. The ‘softer’ PID parameters were applied ($K_{pv} = 0.2$, $K_{iv} = 0.16$, $K_{dv} = 4.8$

for downward or K_{dv} = 1.2 for upward movement) compared to those of experiments 1-3. These parameters were predetermined within the numerical experiments.

Observations/conclusions: it can be seen that the blimp reaches the given altitude very smoothly and does not cross a given point very much. Of course, the time necessary to reach the given altitude is much longer compared to those from Experiments 2 and 3.

5) Autonomous altitude control (with tape measurements) [video: 5_AutoHeightWithTape]

In this experiment, the blimp hovers at a specified altitude and the vertical position of it is measured. The same PID parameters as in experiment 1.

Observations/conclusions: We can observe that the good balanced blimp is able to hover very well within 4-5 [cm].

6) Autonomous flying up and down [video: 6_AutoHeight_125_225]

In this experiment, the flies fly up and down between altitudes of 1.25 and 2.25 [m]. The same PID parameters as in experiment 1.

Observations/conclusions: it was observed that the blimp is well balanced. It crosses the specified altitudes, oscillates little and hovers quite well.

7) Manual position control with autonomous altitude control [video: 7_AutoHeightManualDirection]

In this experiment, the horizontal movement of the blimp is controlled manually by the operator, but the given altitude is controlled simultaneously autonomously. The same PID parameters as in experiment 1.

Observations/conclusions: we can observe that the altitude is controlled autonomously quite well. Of course, because of the more dynamic overall behavior of the blimp, we can see that the blimp dives during turns, but it defends itself against hitting the surface of ice rink.

6.3. Experimental verification of autonomous movement of the blimp to the selected target point

When the altitude controller was finished, then the position controller was developed. To this end, the simplified rule-based controller was implemented and verified. In the near future, the elaborated PID position controller (see Section 1) will be implemented. For all of these experiments, a target point was defined with coordinates: 50.2872338504249° (latitude), 18.6871733366383° (longitude) – this is a center of the ice rink (see a traffic bollard in Fig. 9).

The exemplary experiments carried out so far are as follows:

1) Autonomous flying to the target point without stopping at this point [video: 8_AutoHeightAutoThroughPoint]

In this experiment, the altitude and position are controlled autonomously. The blimp flies to the given target (center of ice rink marked with a traffic bollard) and does not stop at this point.

Observations/conclusions: When the blimp reaches the target point (within a dead zone of radius 3 [m]) it stops the horizontal propellers and flies further due to its inertia. As a consequence, it flies through the target and then turns back. This behavior repeats over and over again – the blimp loiters.

2) 10) Autonomous flying to target point with a stop at this point (example 1, example 2) [videos: 9_AutoHeightAutoToPoint1, 10_AutoHeightAutoToPoint2]
3) In this experiment, the altitude and position are controlled autonomously. The blimp flies to the given target (center of ice-rink marked with traffic bollard) and stops at this point.

4) Observations/conclusions: we can observe that the blimp is able to reach the target point and simultaneously maintain the altitude.

Fig. 9. Blimp reaching a target point (traffic buoy located in the center of the ice rink)

7. CONCLUSIONS

The experiments carried out provided valuable information on the behavior and control of an aerial blimp, leading to several key conclusions. First, the data acquired from real-world experiments proved crucial for accurately tuning the parameters of the developed numerical model of the blimp. This alignment between the simulated and physical systems is essential for reliable virtual testing and control strategy development. Second, the use of this validated numerical model significantly reduced the time and resources typically associated with the development and implementation of a control strategy. By allowing for virtual experimentation and refinement, the model simplified the overall process.

Observations of the numerical model's responses to defined drive controller settings demonstrated that the blimp's movement trajectories are predictable and the quality of these responses was deemed satisfactory. This predictability is a fundamental requirement for designing effective control algorithms. Furthermore, the experiments highlighted the importance of proper balance to maintain a consistent altitude. An imbalanced blimp requires continuous control adjustments to counteract unwanted vertical movement.

Interestingly, it was observed that even when subjected to disturbances causing rotation along the pitch axis, the blimp could maintain its altitude. This inherent stability in the vertical plane under pitch perturbations is a noteworthy characteristic. The potential benefit of independently controlling vertical propellers was also recognized, as this could mitigate unwanted rotation around the pitch axis, leading to more stable and precise vertical control.

Currently, the real blimp's position is managed by a straightforward rule-based controller, which performs adequately. However, based on the promising results obtained from numerical experiments with a PID (Proportional-Integral-Derivative) controller, it is anticipated that implementing this more sophisticated control algorithm on the physical blimp will lead to even better performance, characterized by enhanced accuracy, stability, and responsiveness in its movements. In summary, the research underscores the value of numerical modeling in the development of the airship control system and identifies key factors and potential improvements to achieve precise and robust blimp control.

Acknowledgments

The project was implemented in cooperation with SkyTech Products sp. z o.o.

References

1. Åman Gustaf. 2021. *Indoor Blimp Control*. Master's Thesis TFRT-6134. Lund, Sweden: Department of Automatic Control, Lund University.
2. Ashraf Muhammad Zahir, Mohammad A. Choudhry. 2013. „Dynamic Modeling of the Airship with Matlab Using Geometrical Aerodynamic Parameters". *Aerospace Science and Technology* 25(1): 56-64. DOI: https://doi.org/10.1016/j.ast.2011.08.014.
3. Binti Nur, Mohd Yunus. 2015. *Control of an Autonomous Blimp for Aerial Surveillance*. Project report. Johor Bahru, Malaysia: Faculty of Electrical Engineering, University Technology Malaysia.
4. Burri Matthias, Laura Gasser, et al. 2013. „Design and control of a spherical omnidirectional blimp". In: *IEEE/RSJ International Conference on Intelligent Robots and Systems*: 1873-1879. Tokyo, Japan. DOI: https://doi.org/10.1109/IROS.2013.6696604.
5. Hickson Henry, Andrew T. Conn, Hemma Philamore. 2025. „BlimpleBee: The Helium Assisted Indoor Inspection Drone". In *Towards Autonomous Robotic Systems: 25th Annual Conference TAROS 2024*: 171-183. London, UK. Berlin-Heidelberg: Springer-Verlag. DOI: https://doi.org/10.1007/978-3-031-72062-8_16.
6. Khoury Gabriel Alexander. 2012. *Airship Technology*. 2nd ed. Cambridge: Cambridge University Press. ISBN: 978-1-107-01970-6.
7. Li Yuwen. 2008. „Dynamics Modeling and Simulation of Flexible Airships". PhD thesis. Montreal, Canada: Department of Mechanical Engineering, McGill University.
8. Liu Yiwei, Zengxi Pan, David Stirling, Fazel Naghdy. 2009. „Control of autonomous airship". In: *IEEE International Conference on Robotics and Biomimetics (ROBIO)*: 2457-2462. Guilin, China. DOI: https://doi.org/10.1109/ROBIO.2009.5420403.
9. Sasidharan Anop, Ratna Kishore Velamati, Akram Mohammad, Sabrina Benaissa. 2024. „Mathematical modeling of a single tethered aerostat using longitudinal stability derivatives". *Scientific Reports* 14: 3697. DOI: https://doi.org/10.1038/s41598-024-53851-1.
10. Sebbane Yasmina Bestaoui. 2012. *Lighter than Air Robots: Guidance and Control of Autonomous Airships*. Dordrecht: Springer. DOI: https://doi.org/10.1007/978-94-007-2663-5.
11. Sharma Suryansh, Mike Verhoeff, Floor Joosen, R.R. Venkatesha Prasad, Salua Hamaza. 2024. „A Morphing Quadrotor-Blimp With Balloon Failure Resilience for Mobile Ecological Sensing". *IEEE Robotics and Automation Letters* 9(7): 6408-6415. DOI: https://doi.org/10.1109/LRA.2024.3406061.

12. Van Asares Anthon, Phil Seon Ko, Joshua Samuel Minlay, Brian Raymund Sarmiento, Alvin Chua. 2019. „Design of an Unmanned Aerial Vehicle Blimp for Indoor Applications". *International Journal of Mechanical Engineering and Robotics Research* 8(1): 157-161. ISSN: 2278-0149. DOI: https://doi.org/10.18178/ijmerr.8.1.157-161.
13. Yamada Manabu, Hiroki Adachi, Yasuyuki Funahashi. 2010. „Robust control of an uncertain underactuated airship with asymptotic rejection against wind disturbance". In: *IEEE International Conference on Control Applications*: 1844-1849. Yokohama, Japan. DOI: https://doi.org/10.1109/CCA.2010.5611226.
14. Yang Yueneng, Wu Jie, Xie Yu, Zheng Wei. 2011. „Dynamics Modeling and Maneuverability Analysis of a Near-Space Earth Observation Platform". In: *Proceedings of the 5th International Conference on Recent Advances in Space Technologies (RAST2011)*: 223-226. Istanbul, Turkey. DOI: https://doi.org/10.1109/RAST.2011.5966828.

Received 26.12.2025; accepted in revised form 05.05.2026